

DC – 65 GHz Characterization of Nanocrystalline Diamond Leaky Film for Reliable RF MEMS Switches

Joolien Chee^{1,3}, Ratnakar Karru^{1,3}, Timothy S. Fisher^{2,3}, and Dimitrios Peroulis^{1,3}

¹School of Electrical and Computer Engineering, Purdue University, West Lafayette, IN 47907, USA

²School of Mechanical Engineering, Purdue University, West Lafayette, IN 47907, USA

³Birck Nanotechnology Center, Purdue University, West Lafayette, IN 47907, USA

joolien@purdue.edu, karru@purdue.edu, tsfisher@purdue.edu, dperouli@purdue.edu

Abstract—This paper reports on the growth, patterning, and characterization of plasma-enhanced chemical vapor deposition (PECVD) thin diamond film for DC-65 GHz applications. Nanocrystalline films are successfully demonstrated with an average grain size of less than 60 nm that can replace conventional low-quality dielectrics in RF MEMS switches. In addition to their excellent surface properties, the diamond film has negligible RF loss up to at least 65 GHz, but non-zero DC conductivity of approximately 0.2 $\mu\text{S}/\text{m}$ that allows the film to provide a conductive path for potential trapped charges. Such films are envisioned to be integrated in today's capacitive RF MEMS switches that suffer from charge-induced stiction.

I. INTRODUCTION

A large number of RF MEMS capacitive switches have been demonstrated over the past decade with undeniable advantages over their solid-state counterparts including very low loss (< 0.2 dB), high isolation (> 30 dB), high linearity (third-order intercept point $> +66$ dBm) and high bandwidth (> 40 GHz) [1]. Nevertheless, dielectric charging is one of the most serious failure mechanisms that hinders their integration into real-life communication systems. Dielectric charging is an electrical phenomenon where charges are injected into, and retained by the dielectric material that lies underneath the suspended switch bridge [2], [3]. Dielectric charging is usually observed as a shift of the $C-V$ curve of the device during the lifetime of the device. Eventually stiction of the device and/or dielectric breakdown may occur.

While a few attempts have been made to mitigate this issue [1], no final answer has been obtained. The most common solution is the usage of bipolar voltage when biasing the MEMS switch. However, charge injection and removal are not identical for positive and negative voltages. In addition, this solution does not account for the possibility of ionizing radiation that is of great interest in satellite and high-amplitude communication systems. Recently, the possibility of using leaky dielectrics has been proposed by [4], [5] as a very promising solution to dielectric charging. The major idea lies on replacing the conventional completely insulating dielectrics (usually Si_3N_4 and SiO_2) with leaky dielectrics that provide a conductive path for the potentially trapped charges. This method may substantially decrease the recombination times for the trapped charges and considerably improve the reliability of the devices.

Practical leaky dielectrics for MEMS switches need to satisfy many requirements including: 1) very low roughness for high on/off capacitance ratios, 2) thickness in the range of 0.1-1 μm , 3) low dielectric loss to retain the inherently high quality of MEMS switches, and 4) non-zero DC conductivity. In this work, we demonstrate for the first time that it is possible

TABLE I
DEPOSITION PARAMETERS OF THE DIAMOND FILM

Process Parameter	BEN	Growth
Gas flow rate ($\text{CH}_4:\text{H}_2$) [sccm]	10:200	2:200
Plasma Power [W]	300	300
Pressure [torr]	15	15
Substrate Bias [V]	-250	-125

TABLE II
PLASMA PATTERNING PARAMETERS

Process Parameter	Passivation	Etch
Gas flow rate [sccm]	O_2 (40)	$\text{SF}_6:\text{O}_2$ (4:40)
Plasma Power [W]	100	200
Pressure [torr]	0.05	0.05
Bias [V]	300	680

to produce nanocrystalline PECVD diamond films that satisfy all these requirements for frequencies as high as 65 GHz. Section II describes the fabrication process of the diamond film and Section III presents the RF and DC experimental results.

II. FABRICATION

The use of diamond as a dielectric material on silicon substrate has been investigated by several researchers, each with varied growth methods and film quality [6]. Plasma-enhanced chemical vapor deposition (PECVD) offers low contaminant concentration, relatively low growth temperatures, predictable film quality, and is compatible with MEMS fabrication processes. Coupled with bias-enhanced nucleation (BEN) [7], [8] smooth films can be produced by reducing the grain size of the diamond crystals.

The films studied in this work were deposited in a microwave plasma CVD system (SEKI AX 5200S) on high-resistivity (>10 $\text{K}\Omega\text{-cm}$) silicon substrates. The deposition consisted of two separate phases; the BEN phase followed by growth phase. A molybdenum holder resting on a graphite susceptor holds the substrate and facilitates the concentration of plasma. No surface treatment was performed on the substrate prior to deposition. Methane and hydrogen were used as source gases. The flow rates were kept constant at 10 and 200 sccm respectively and the pressure in the chamber was maintained at 15 torr during the BEN phase. Methane flow rate was reduced to 2 sccm during growth phase. The graphite susceptor was inductively heated to keep the substrate temperature at 700°C during the entire deposition. Deposition durations ranging from 30 minutes to over 8 hours have been

successfully carried out under 300 W plasma generated by an ASTeX 2.45 GHz (AX2115) microwave source. A variety of film thicknesses ranging from 0.3 to over 15 μm have been obtained. A constant DC bias of -250 V and -125V was applied to the substrate throughout the BEN phase and growth phase, respectively, to facilitate a uniform film growth on the substrate. Table I summarizes the BEN phase and growth phase parameters.

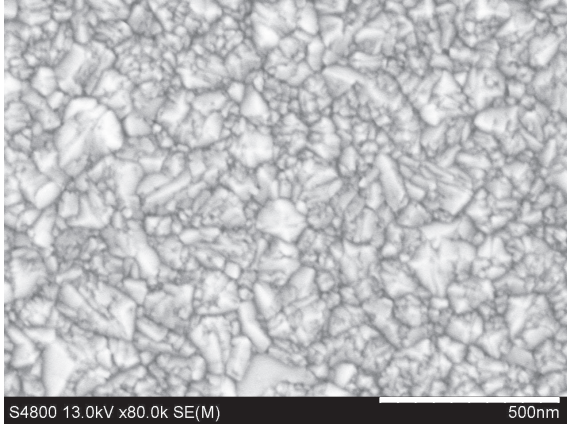


Fig. 1. SEM picture of a nanocrystalline diamond film.

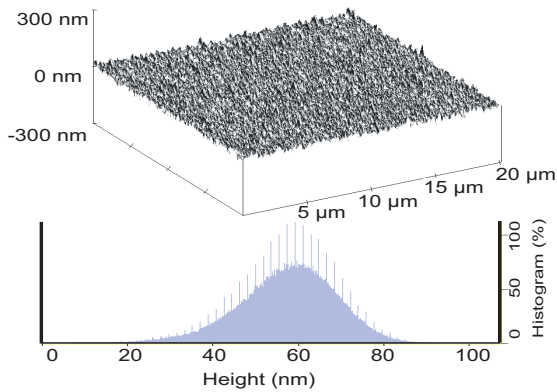


Fig. 2. AFM image of nanocrystalline diamond film surface. The histogram presents the grain size distribution.

To incorporate the diamond film into MEMS devices, a patterning process utilizing plasma etch was developed. 1 μm evaporated aluminum was first deposited over the diamond film and subsequently patterned to serve as the plasma etch mask. Plasma etch was performed in a Plasma Technology RIE using parameters from Table II. Passivation of the aluminum mask in an oxygen-rich, low-power plasma environment prior to diamond etch increases the mask-to-target etch ratio. The diamond film was etched in $\text{SF}_6:\text{O}_2$ plasma with an etch rate of approximately 45 nm/minute. Fig. 1 and Fig. 2 shows the SEM and AFM image of the deposited nanocrystalline diamond film surface. The average grain size is approximately 60 nm, with size ranging from 40 to 80 nm. The AFM image (Fig. 3) shows the 3-dimension edge profile of the plasma-etched diamond film. The film thickness was 1.4 μm and was deposited using 1 hour BEN followed by 3 hours growth. This film deposition condition was repeated for fabrication of both RF and DC test devices.

Fig. 4 shows the Raman spectrum of the diamond film obtained. Measurements were performed at room temperature

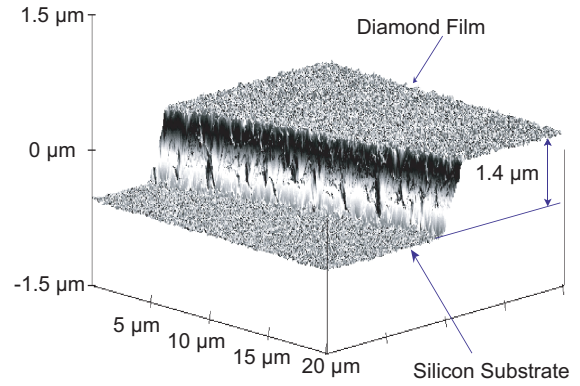


Fig. 3. AFM image of 1.4 μm diamond film etched in plasma environment. The higher surface shows the roughness of the original diamond film, while the lower surface is the silicon substrate.

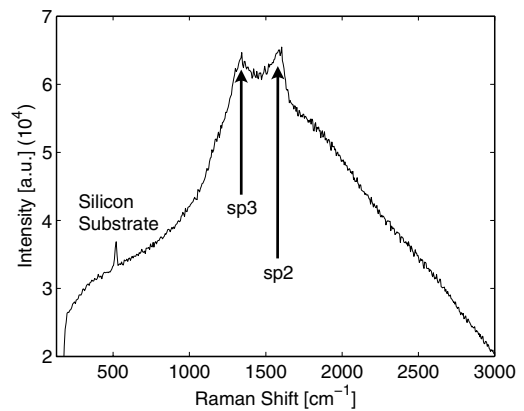


Fig. 4. Raman spectrum of deposited diamond film.

using a Helium-Neon laser (632.8 nm, 50mW) as the excitation source. The spectrometer was calibrated using an Argon-Neon lamp and the software package WINSPEC was used to evaluate the spectra. A sharp peak at 520 cm^{-1} was observed in Fig. 4 along with two broad peaks at 1332 cm^{-1} and 1580 cm^{-1} . The 520 cm^{-1} peak is due to the silicon substrate. The peak at 1580 cm^{-1} (G-peak) indicates the presence of sp^2 bonded carbon while the peak at 1332 cm^{-1} is attributed to sp^3 bonded carbon [9]. The composition of diamond- and graphite-like film demonstrates two desirable characteristics; material hardness and electrical conductivity.

III. RF AND DC MEASUREMENTS

Two of the desired properties of this film are low RF loss and non-zero DC conductivity. As already mentioned before, the low RF loss is required for high-Q MEMS switches and varactors, while the non-zero DC conductivity is needed to provide a conducting path for the trapped charges to escape from the film.

The RF loss was characterized by comparing the RF performance of coplanar waveguide (CPW) lines (Fig. 5) printed on three different materials. The lines were 1.24 cm long, 50/80/50 μm CPW made of evaporated Ti/Au (0.1/1 μm) on (i) 1.4 μm diamond film on high-resistive ($>10 \text{ K}\Omega\text{-cm}$) silicon substrate, (ii) 0.5 μm thermally-grown silicon dioxide film on high-resistive silicon substrate, and (iii) high-resistive silicon substrate. All measurements were performed on the Agilent 8510XF network analyzer using on-wafer probes and standard

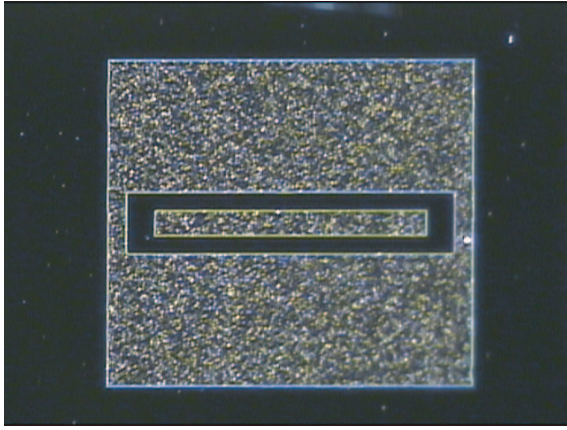


Fig. 5. Microphotograph of a Ti/Au coplanar waveguide line printed on a $1.4 \mu\text{m}$ diamond film on a $550 \mu\text{m}$ thick $>10 \text{K}\Omega\text{-cm}$ silicon substrate. The line length in the picture is $820 \mu\text{m}$.

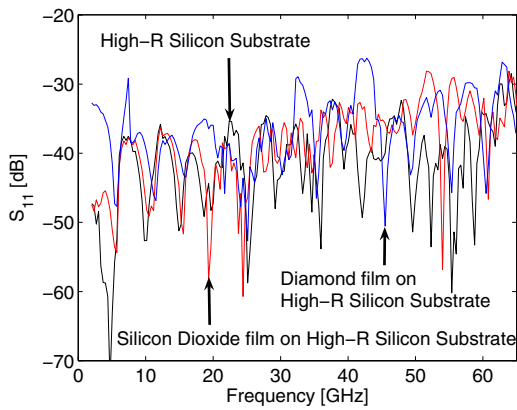


Fig. 6. Measured reflection loss of 1.24-cm transmission line printed on diamond film and on silicon dioxide. Both films were deposited on $>10 \text{K}\Omega\text{-cm}$ silicon substrates. A similar 1.24-cm transmission line was also printed on silicon substrate.

TRL calibration. Fig. 6 and Fig. 7 show the measured return and insertion losses. The return loss for all three material configurations was less than -25 dB from DC to 65 GHz. The insertion loss at 30 GHz for (i), (ii), and (iii) was 1.7, 1.8 and 1.4 dB/cm respectively. Table III presents the loss for all three materials at 10, 30, and 65 GHz.

The DC conductivity of the film was determined by first fabricating a diamond film resistor and then performing post-measurement simulations of the model. The device (Fig. 8) had a $1.4 \mu\text{m}$ -thick diamond film sandwiched between two metal contact pads. The bottom and top contacts were Cr/Pt ($0.03/0.3 \mu\text{m}$) and Ti/Au ($0.1/1 \mu\text{m}$). The average resistance of the diamond film was approximately $70 \text{ M}\Omega$, while that of the Cr/Pt and Ti/Au contacts was 6Ω and 0.5Ω , respectively. HP 34401A digital multi-meter was employed to measure all

TABLE III
INSERTION LOSS OF CPW ON THREE MATERIAL CONFIGURATIONS.

Frequency (GHz)	(i)* (dB/cm)	(ii)* (dB/cm)	(iii)* (dB/cm)
10	1.2	1.4	1.0
30	1.7	1.8	1.4
65	2.6	2.3	2.1

*See text for details.

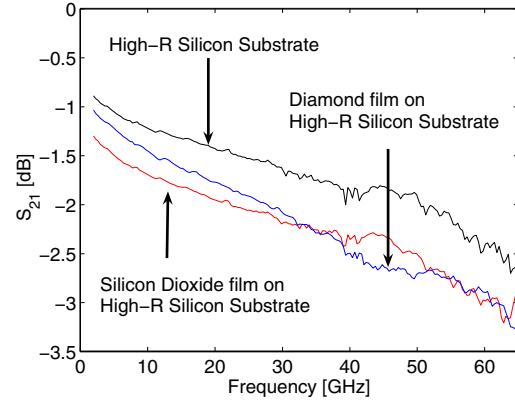


Fig. 7. Measured insertion loss of 1.24-cm transmission line printed on diamond film and on silicon dioxide. Both films were deposited on $>10 \text{K}\Omega\text{-cm}$ silicon substrates. A similar 1.24-cm transmission line was also printed on silicon substrate.

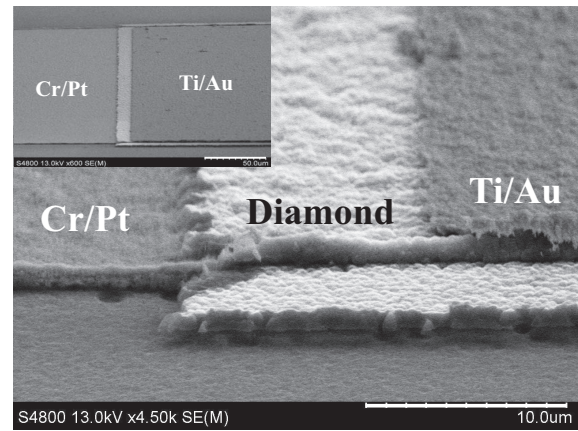


Fig. 8. SEM picture of $1.4 \mu\text{m}$ -thick diamond film sandwiched between Cr/Pt and Ti/Au metal contact pads. Insert is a larger view of the same device.

resistances. The $600 \mu\text{m} \times 300 \mu\text{m}$ Cr/Pt contact was first evaporated and patterned using photoresist lift-off technique. The diamond film was later grown above the Cr/Pt pads and patterned into $300 \mu\text{m}$ squares utilizing the PECVD deposition and plasma etch techniques described earlier. The top $600 \mu\text{m} \times 300 \mu\text{m}$ Ti/Au pad was then evaporated and subsequently wet etched. Ansoft Maxwell SV [11] simulation software was utilized to match the measured resistance by varying the intrinsic material conductivity. Conductivity was assumed to be isotropic, linear, and homogeneous. Maxwell SV computed the two-dimensional spatial current density in the diamond film. The resistance was then determined by integrating the total current between the contacts. Voltage potential between the two contacts was kept constant throughout the modelling. The calculated conductivity of the diamond film was approximately $0.2 \mu\text{S/m}$ and is nine orders magnitude larger than that of silicon dioxide and silicon nitride films grown in PECVD environment. Both silicon-based dielectrics have conductivity of $<10^{-16} \text{ S/m}$ [1]. This charge-leaky property could alleviate dielectric charging problems and significantly improve the lifetime of the RF MEMS switches and varactors.

IV. CONCLUSION

We have characterized for the first time nanocrystalline diamond thin films for RF MEMS applications from DC to 65 GHz. Also demonstrated were the deposition of 60 nm size

diamond crystals and patterning techniques. While these films have proven to introduce no additional RF loss, their non-zero DC conductivity allows them to be used as high-quality leaky dielectric films in RF MEMS switches. Such films have the potential to substantially improve the reliability of existing RF MEMS switches because they can alleviate the trapped-charge induced stiction.

V. ACKNOWLEDGEMENT

This work has been generously supported by the Multifunctional Adaptive Radio, Radar and Sensors (MARRS) MURI Project (Award Reference Number 2001-0694-02).

REFERENCES

- [1] G. M. Rebeiz, "RF MEMS, theory, design and technology", *John Wiley and Sons*, 2003.
- [2] C. Goldsmith, J. Ehmke, A. Malczewski, B. Pillans, S. Eshelman, Z. Yao, J. Brank, M. Eberly, "Lifetime characterization of capacitive RF MEMS switches", *2001 IEEE MTT-S International Microwave Symposium Digest*, vol. 1, 2001, pp. 227-230.
- [3] J. R. Reid, L. A. Starman, R. T. Webster, "RF actuation of capacitive MEMS switches", *2003 IEEE MTT-S International Microwave Symposium Digest*, vol. 3, 2003, pp. 1919 - 1922.
- [4] J. P. Sullivan, T.A. Friedmann, K. Hjort, "Diamond and amorphous carbon MEMS", *Materials Research Society Bulletin*, vol. 26, no. 4, 2001, pp. 309-311.
- [5] J. R. Webster, C. W. Dyck, J. P. Sullivan, T.A. Friedmann, A. J. Carton, "Performance of amorphous diamond RF MEMS capacitive switch", *Electronics Letters*, vol. 40, no. 1, 2004, pp. 43-44.
- [6] P. May, "Diamond thin films: a 21st-century material", *Philosophical Transactions Royal Society London A*, vol. 358, 2000, pp. 473-495.
- [7] Y. Gurbuz, W. P. Kang, J. L. Davidson, D. V. Kerns, Q. Zhou, "PECVD Diamond-Based High Performance Power Diodes", *IEEE Transactions on Power Electronics*, vol. 20, no. 1, 2005, pp. 1-10.
- [8] J. Robertson, J. Gerber, S. Sattel, M. Weiler, K. Jung, H. Ehrhardt, "Mechanism of bias-enhanced nucleation of diamond on Si", *Applied Physics Letters*, vol. 66, no. 24, 1995, pp. 3287-3289.
- [9] W. J. Yang, Y.H. Choa, T. Sekino, K. B. Shim, K. Nihara, K. H. Auh, "Structural characteristics of diamond-like nanocomposite films grown by PECVD", *Materials Letters*, vol. 57, no. 21, 2003, pp. 3305-3310.
- [10] J. B. Muldavin, G. M. Rebeiz, "High-isolation CPW MEMS shunt switches - I. Modeling", *IEEE MTT Transactions on Microwave Theory and Techniques*, vol. 48, no. 6, 2000, pp. 1045-1052.
- [11] Ansoft Corporation, Maxwell 2D Student Version (Maxwell SV), <http://www.ansoft.com>